Nanoscale

Probing the Effect of Surface Chemistry on the Electrical Properties of Ultrathin Gold Nanowire Sensors

Journal:	*Nanoscale*
Manuscript ID:	NR-ART-11-2013-005927.R1
Article Type:	Paper
Date Submitted by the Author:	07-Nov-2013
Complete List of Authors:	kisner, Alexandre; Rutgers University, Heggen, Marc; Peter Grünberg Institut-5, Forschungszentrum Jülich GmbH, 52425 Jülich, Germany, Mayer, Dirk; Peter Grünberg Institut-8, Forschungszentrum Jülich GmbH, 52425 Jülich, Germany, Simon, Ulrich; Institute of Inorganic Chemistry, RWTH Aachen University, Landoltweg 1, 52074 Aachen, Offenhausser, Andreas; Forschungszentrum Julich, Inst. Bio- and Nanosystems Mourzina, Yulia; Research Centre Juelich,

Cite this: DOI: 10.1039/c0xx00000x

www.rsc.org/xxxxxx

ARTICLE TYPE

Probing the Effect of Surface Chemistry on the Electrical Properties of Ultrathin Gold Nanowire Sensors

Alexandre Kisner,*[‡ab] Marc Heggen,[c] Dirk Mayer,[ab] Ulrich Simon,[bd] Andreas Offenhäusser[ab] and Yulia Mourzina*[ab]

Received (in XXX, XXX) Xth XXXXXXXXX 20XX, Accepted Xth XXXXXXXXX 20XX
DOI: 10.1039/b000000x

Ultrathin metal nanowires are ultimately analytical tools that can be used to survey the interfacial properties of the functional groups of organic molecules immobilized on nanoelectrodes. The high ratio of surface to bulk atoms makes such ultrathin nanowires extremely electrically sensitive to adsorbates and their charge and/or polarity, although little is known about the nature of surface chemistry interactions on metallic ultrathin nanowires. Here we report the first studies about the effect of functional groups of short-chain alkanethiol molecules on the electrical resistance of ultrathin gold nanowires. We fabricated ultrathin nanowire electrical sensors based on chemiresistors using conventional microfabrication techniques, so that the contact areas were passivated to leave only the surface of the nanowires exposed to the environment. By immobilizing alkanethiol molecules with head groups such as $–CH_3$, $–NH_2$ and –COOH on gold nanowires, we examined how the charge proximity due to protonation/deprotonation of the functional groups affects the resistance of the sensors. Electrical measurements in air and in water only indicate that beyond the gold-sulfur moiety interactions, the interfacial charge due to the acid-base chemistry of the functional groups of the molecules has a significant impact on the electrical resistance of the wires. Our data demonstrate that the degree of dissociation of the corresponding functional groups plays a major role in enhancing the surface-sensitive resistivity of the nanowires. These results stress the importance of recognizing the effect of protonation/deprotonation of the surface chemistry on the resulting electrical sensitivity of ultrathin metal nanowires and the applicability of such sensors for studying interfacial properties using electrodes of comparable size to the electrochemical double layer.

1 Introduction

Chemical sensing based on the conductance change of one-dimensional (1D) nanostructures such as nanowires (NWs) and/or nanotubes (NTs) is a highly innovative and application-oriented field of research, since it promises rapid, label-free and highly sensitive detection by this new and powerful class of sensors.[1-5] To date, significant progress has been achieved in the development of 1D sensors based on carbon nanotubes and silicon NW transistors.[6,7] Although less frequently exploited as sensing nanostructures, devices based on noble metal NWs are also very interesting for NW-based sensors due to the sensitive change in charge transport and electrochemical properties caused by surface adsorbates.[8-10] Hence, when the diameter of NWs approaches a few nanometers (ultrathin nanowires), the adsorption of a small number of molecules on the surface of the NWs significantly increases electrical resistance. This allows minute concentrations of a specific analyte to be probed, which can even approach the single-molecule level.

Previous studies of metallic NWs applied as chemiresistors have demonstrated different device configuration and mechanisms of sensing. For instance, the pioneering work by Tao et al. introduced atomically thin metal wires, in which the conductance is quantized and strongly influenced by the interaction strength of molecules adsorbed on their surface.[11-14] The sensing response in this case, i.e., the conductance change upon molecule adsorption, is attributed to atomic rearrangements and the mechanical stability of quantum wires. Bohn and co-workers succeeded in fabricating gold nanowires (AuNWs) either by electron beam lithography or focused ion beam (FIB) milling.[15] They found that due to the reduced grain size and lattice damage caused by the ion milling process, NWs produced by FIB exhibit a lower sensitivity. Other groups have also developed chemiresistors based on metal NWs and NTs fabricated by nanoskiving, electrodeposition and atomic force microscopy nanoscratching followed by metal coating.[16-19] Although these approaches have provided fundamental insights into mechanisms of sensing resistance changes, apart from the work of Tao's group, in all other cases the sensor performance is limited by the polycrystalline nature and thus by grain boundary effects. Therefore single-crystalline metal NWs would be highly desirable building blocks for advanced chemiresistors, both from the scientific as well as from the technological point of view.

More recently, the synthesis of single-crystalline ultrathin Au NWs presenting diameters of around 2 nm and lengths of several micrometers was reported.[20-25] The diameters of such nanowires approach those of molecules and their aspect ratio (length/diameter) is extraordinarily high enabling them to be contacted by microstructured electrodes. Similarly to the advances made in the knowledge of the interfacial chemistry of devices based on silicon nanowires and carbon nanotubes, it is thus expected that significant progress can also be made in the field by applying such NWs as chemiresistors.[26-30] Since long ultrathin metal NWs are almost completely composed of surface atoms and their surface topography and roughness differs significantly from polycrystalline nanowires, a comprehensive study of the surface chemistry and interfacial charge of adsorbed molecules is central for understanding surface sensitive resistivity at the nanowire-liquid interface and will provide unique information for sensing mechanisms.

Here, we describe the fabrication of chemiresistors using ultrathin single-crystalline Au NWs. These AuNWs are contacted by means of photolithography, whereas the contact areas were protected in order to avoid effects arising from adsorption at the contacts. This allows us to restrict the monitoring of the sensor response to the nanowire surface exposed to the liquid phase. By applying short-chain alkanethiol molecules with different functional groups in air and in water, we systematically studied the molecular sensing properties. In particular, we evaluated the effect of the protonation/deprotonation of the head groups of immobilized molecules in close proximity to the metal on the surface sensitive resistivity of the NWs. Our results show that besides the Au-binding moiety of the molecules, their interfacial charge due to acid/base dissociation in solution has a significant impact on the electrical resistance of the wires, which may dramatically enhance this effect, depending on the chemical functionality. As a result, these investigations demonstrate the influence of the acid-base properties of immobilized molecules on the electrical sensitivity of ultrathin AuNWs, thus highlighting the importance of the protonation/deprotonation equilibrium of the surface chemistry when designing new sensors based on such wires.

2 Experimental

2.1 Synthesis of Nanowires

The chemicals employed in the synthesis were all purchased from Sigma-Aldrich and were used as received. The ultrathin Au NWs were produced employing a synthesis methodology described elsewhere.[25] In brief, AuCl (7.4 mg) was dissolved in a round-bottom flask using oleylamine (10 mL) and hexane (1 mL) and the reaction was left to rest without agitation at room temperature for 24 h. The solution was then heated to 80 °C for 6 h, and O_2 (99.998% from Praxair) was bubbled into the solution during this period. Upon completion of the reaction, the Au NWs were precipitated out with ethanol (~5 mL), followed by centrifugation (12000 rpm, 20 min). Finally, the supernatant was removed and the precipitate containing the NWs was dispersed in hexane. This centrifugation step was repeated three times.

2.2 Electron Microscopy Analysis

Transmission electron microscopy (TEM) analyses were carried out with an FEI CM20 and an FEI Technai F20 transmission electron microscope, both operated at 200 kV. The samples were prepared by drop casting a solution of the nanowires dispersed in hexane over copper grids coated with Formvar and carbon film (Plano GmbH). Scanning electron microscopy (SEM) images were obtained using a field-emission SEM JEOL JSM 6330F.

2.3 Device Fabrication

The electrodes designed to contact the Au NWs were fabricated using a conventional photolithography process. Briefly, the photoresist AZ 5214 was spun at 4000 rpm over a silicon substrate with 400 nm thermal SiO_2 on the surface. A photolithography step where the substrates were exposed to the UV-vis light (365 nm) for 6 s was then performed. Afterwards, a post-bake process at 130 °C for 75 s, followed by the development of the photoresist for 50 s in the metal-ion-free 326 (MIF 326) solution, was carried out. This opened the lanes to deposit the metal electrodes and the contact pads. The devices were fabricated by depositing 10 nm of Ti and 100 nm of Au by electron beam evaporation and a lift-off process in acetone was then performed to remove the photoresist (Figure 2A). The distance between the electrodes was 3 μm.

2.4 Fluid-Directed Assembly of Au NWs on the Device

In order to electrically characterize the NWs they had to be assembled over at least two electrodes previously fabricated by photolithography. To accomplish this, we employed a solution of Au NWs (~1 mg/mL) dispersed in hexane and exposed it to ultra-sound for about 10-15 s. In the next step, ~ 20 μL of the ultra-sonicated solution was passed inside a poly(dimethylsiloxane) (PDMS) microfluidic channel previously aligned over the metal leads (Figure 2B). Due to the shear and normal forces acting during the flow process, the NWs were then aligned in the flow direction and immobilized via the van der Waals interaction between the electrodes (Figure 2C). As the PDMS mold is not covalently sealed through -O-Si-O- bonds on the substrate, it allows the microfluidic channel to be removed after each set of experiments and reused for the same or other substrates.

2.5 Passivation of Au NW Devices

After deposition of the Au NWs, the passivation of the metallic electrodes was performed by covering the whole surface with a layer of about 220 nm of PMMA (polymethyl methacrylate) 600 K, which was spun at 4000 rpm. The areas of the contact pads between the pair of electrodes containing the NWs were then patterned by electron-beam lithography using a dose of 300 μC/cm^2. The PMMA was developed for 1 min using the PMMA developer 600-55 K, followed by submersion of the sample in iso-propanol for 30 s and drying in nitrogen (N_2). This step generated channels (grooves) between the pair of electrodes, leaving the surface of the assembled NWs exposed to the environment (Figure 2D). Additionally, the removal of PMMA from the contact pads allowed them to be electrically contacted

by external sources.

2.6 Current–Voltage Measurements

The assembled nanowires were electrically characterized by a Keithley semiconductor analyzer (model 4200 SCS). The leads were electrically contacted through the bond pads using tungsten needles. The main electrical characterization was based on a two-point probe measurement, where DC voltages were applied and the resulting current was measured, i.e. current-voltage (I–V) measurements (DC bias). The resistance of the NWs was then calculated from the I–V curves.

2.7 Surface Modification of Au NW Devices with Alkanethiols

The surface of Au NWs was modified with three different kinds of alkanethiol molecules, i. e., 1-mercapto-propane (thiolpropane, TP), mercapto-propionic acid (MPA) and cysteamine (CA). All the alkanethiols were purchased from Sigma-Aldrich and had a purity > 98.0%. Solutions with different concentrations of the respective alkanethiols were prepared in absolute ethanol (Merck). The surface modification of Au NWs was performed by exposing the central area of the devices to the alkanethiol solutions for 10 min. Afterwards, the devices were first washed with absolute ethanol and then rinsed with Milli-Q water and dried with a stream of Ar. The electrical characterization of the modified Au NWs was also carried out using the Keithley semiconductor analyzer (model 4200 SCS). I–V measurements were made in air and also with the surface of the devices covered with a drop (~ 150 µL) of Milli-Q water 18 MΩ, pH 6.7.

2.8 Zeta Potential Measurements

Zeta potential measurements were carried out in order to estimate the surface potential generated by the adsorption of such alkanethiol molecules on nanowires. In doing so, Au NWs dispersed in hexane were centrifuged for 15 min at 20000 rpm. Afterwards, the supernatant was removed and 10 mmol L^{-1} of alkanethiol solution prepared in absolute ethanol was added to the NWs precipitated in the bottom of the flask. After 10 min the alkanethiol solution was removed and the wires were washed twice with pure Milli-Q water before zeta potential measurements. A Malvern ZetaSizer 4 equipped with a LaserZee Meter (Pen Kem Model 501) was then used for the zeta potential measurements. For each sample, 5 independent measurements were performed. All data were recorded at 20 °C.

3 Results and Discussion

Figure 1 shows the transmission electron micrograph of a representative parallel array of co-synthesized NWs. The NWs exhibit a mean diameter of about 2 nm and can be several micrometers long, which means that their aspect ratios may be as high as several thousands. Gold nanoparticles and a few thicker NWs co-produced during the synthesis can also be seen in the micrograph.

We note that unlike other ultrathin NWs, which are unstable in environmental conditions, these Au wires persist for several

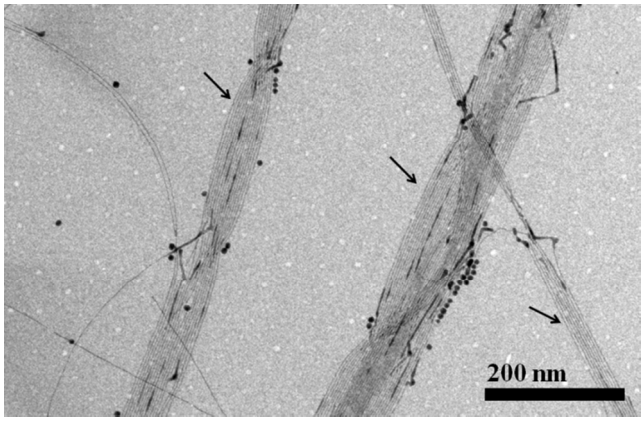

Fig. 1 Transmission electron micrograph of the ultrathin Au NWs (indicated by the arrows).

months in solution. Specifically, the ultrathin NWs can be stored and well dispersed in hydrophobic organic solvents of linear alkyl chains such as hexane.

To configure the ultrathin Au NWs as chemiresistors, they have to be electrically contacted at the ends by means of two electrodes. The basic steps for fabricating these devices are described in the experimental section and shown in Figure 2.

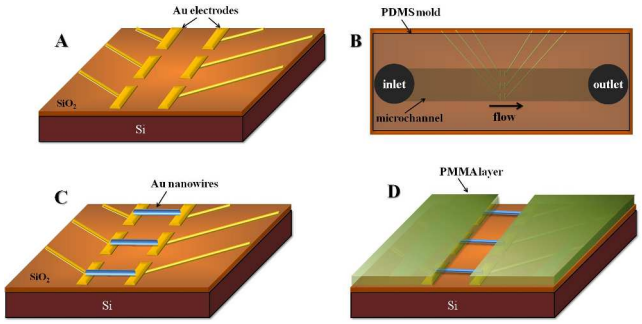

Fig. 2 Schematic of the basic steps for fabricating the chemiresistors including: A) thermal oxidation of the Si substrate followed by a conventional photolithography step and Ti/Au (10/100 nm) metal deposition and lift-off process. B) A PDMS mold containing a microchannel is aligned and brought into contact with the surface of the substrate where the Au electrodes were previously fabricated. C) The NWs are assembled between the pair of Au electrodes by passing a NW suspension inside the microchannel. D) Passivation of the contact areas of the devices by depositing and patterning a PMMA layer employing electron-beam lithography. This final step left only the surface of the NWs exposed to the environment.

Before surface modification of NWs with different alkanethiols, the co-produced devices were characterized by current versus voltage (I–V) measurements in air. Figure 3A shows an SEM image of a bundle of Au NW devices passivated with PMMA, while Figure 3B displays its I–V curve exhibiting linear behavior. The calculated resistance from the least squares method for this device was 6.7 MΩ. As a whole, the electrical resistance of more than 60 Au NW devices was around 1 – 10 MΩ, with a predominance of wires having a resistance of 1.3 MΩ (inset Figure 3B).

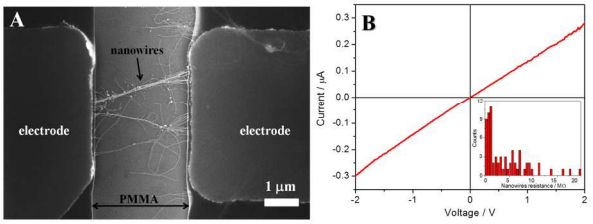

Fig. 3 A) Scanning electron microscopy image of a typical Au NW chemiresistor. The NWs were assembled over a pair of electrodes passivated with PMMA. B) Current vs voltage of a Au NW device with an electrical resistance of ≈ 6.7 MΩ. The inset at the bottom right shows a histogram of electrical resistance values of 65 NW devices.

This range of variation in the resistance of the devices can be partially associated with a variance in the number of nanowires on the bundle assembled between the electrodes. In average the bundles contacting the electrodes were composed by about 20-30 Au NWs. It is important to recognize that single Au NW devices can be produced by reducing the concentration of nanowires in the dispersion that is flow over the metal electrodes using the microfluidic channel (data not shown). The measured resistances of the devices are comparable to the results obtained by Chandni *et al.*, who also fabricated devices based on ultrathin Au NWs synthesized in a similar manner to the NWs produced in this work.[31]

This relatively high resistance is primarily attributed to the contact resistance between NWs and electrodes, as already observed in our previous investigation.[32] Also, it is important to take into account the fact that the nanowires exhibit diameters smaller than the mean free path of the conduction electrons (for Au, ≈ 80 nm).[33] Thus it can be expected that the effects of surface scattering additionally contribute to the high resistivity observed. These results highlight the importance of passivating the contact areas to leave only the surface of the NWs exposed to the environment.

In order to understand the effect of surface chemistry on the electrical properties of the Au NWs, we immobilized alkanethiol molecules with different functional groups on their surface and measured the corresponding electrical characteristics in air and aqueous media. The molecules immobilized on Au NWs were thiolpropane, cysteamine and mercapto-propionic acid (Figure 4A). The choice of these molecules was firstly based on the thermodynamically favorable covalent interaction of the thiol functional group with Au and consequent formation of self-assembled monolayers (SAMs) on its surface.[34] Secondly, their short and similar lengths in the range of 4–8 Å create a barrier where the aqueous double layer forms.[35,36] Thirdly, the charge of their functional groups is favorable when the molecules are in aqueous media near pH 7.0. In this case, the immobilization of MPA molecules on Au NWs could generate a net of negative charges due to the deprotonation of their carboxyl groups, while on the other hand CA could yield a positively charged surface due to protonation of their primary amine groups and TP would serve as a non-charged or neutral molecule (Figure 4A). Our key concept in these experiments was to observe the effect of the

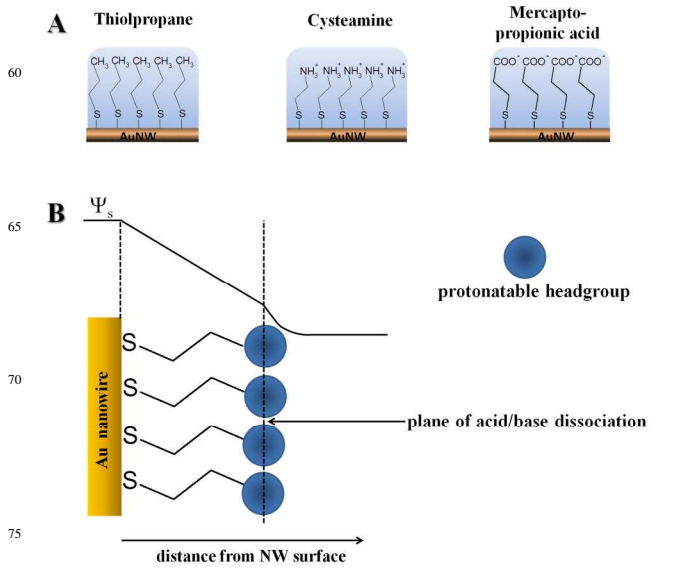

Fig. 4 A) Chemical structure of the alkanethiol molecules immobilized on Au NWs and their corresponding expected ionization state in aqueous solution with pH near 7. B) Schematic illustrating the Au NW/SAM/aqueous interfacial region.

metal surface potential on the acid-base chemistry of the functional groups of the molecules, which form a plane of dissociation on the boundary with the diffuse aqueous double layer (Figure 4B). The protonatable head groups of the molecules are 5-6 Å beyond the NW surface and hence the metal surface can experience the interfacial electric field strength provided by the charges of the ionized groups and the functional groups of the molecules can sample the electric field strength from the applied potential in the NWs.

The responses (I –V curves) in air and in water of three representative Au NW devices before and after their modification with different concentrations of TP, MPA and CA are given in Figures 5A-F, respectively.

The measured curves show some common general aspects. First, in all cases the NW devices presented a systematic increase in the electrical resistance with increasing concentration of the alkanethiol solution. This effect was observed even when concentrations as low as 10 μmol L^{-1} were employed and indicates the binding of the respective thiol molecules on the surface of Au NWs. Second, most of the I–V curves from the measured devices presented a transition from linear to quasi-linear when alkanethiols were immobilized on the NW surface. Third, the curves measured in aqueous solution exhibited hysteresis and the hysteresis effect was more pronounced on those NW devices where MPA was immobilized. We will start by discussing the increase in the electrical resistance of the NWs upon adsorption of alkanethiols. A summary of the results for variations in the electrical resistance of the NWs before and after immobilization of the molecules shown in Figures 5A-F is presented in Table 1. These results are based on measurements that were carried out in different devices and expressed in terms of relative variation before and after their chemical functionalization, thus compensating the error due to variations in the intrinsic electrical resistance of the devices. The data of the measurements in air demonstrate an increase in concentration-

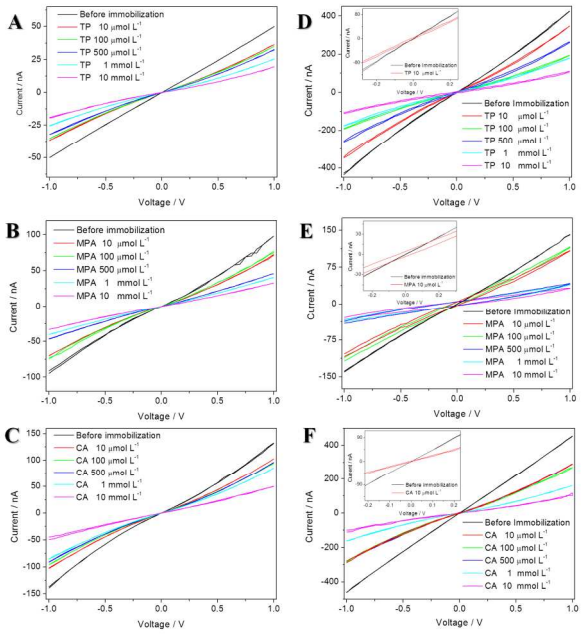

Fig. 5 Electrical characteristics in air (Figs. A, B and C) and in aqueous solution (Figs. D, E and F) of Au NW devices before and after their surface modification with variable concentrations of thiolpropane (A and D), mercapto-propionic acid (B and E) and cysteamine (C and F), respectively. All the curves were recorded in a sweeping mode. The upper left insets in Figures D, E and F show a zoom of the I – V behavior near 0 V of the Au NW devices measured in water before and after their surface modification with 10 μmol L^{-1} of the respective organothiol.

dependent resistance behavior with a notable increase of more than 30% in the resistance of the NWs when the devices were exposed to only 10 μmol L^{-1} of TP, MPA and CA. Additionally, a remarkable change of over 100% in the resistance of the NWs was observed when 10 mmol L^{-1} of the respective organothiols was employed. In comparison, the data of the measurements with the devices submerged in water show that the increase of the NW resistance in all the applied concentrations of thiols was substantially higher than that measured in air. In the case of NWs exposed to 10 mmol L^{-1} of MPA and CA, the resistance increased a few hundred-fold. We attributed this increase in the resistance of the wires to the thiol binding rather than to the growth of oxide layers on their surface during the measurements in aqueous media. This hypothesis was verified by measuring the same resistance of the wires in air before and after recording their I–V curves in water (Figure S1, supporting information). Thus, these results readily demonstrate the high sensitivity of the wires to small thiol adsorbates in both dry and wet conditions.

The change in the resistance of ultrathin metal NWs can be understood in a similar way for ultrathin metal films. In the case of nanowires, especially those that are ultrathin, most of atoms are on the surface and as the lateral dimensions of the NWs are much smaller than the mean free path of conduction electrons, and their surface contributes significantly to the electron scattering and to the NW resistance. This means that the adsorption or the binding of molecules to the surface of such NWs can drastically affect the conduction electrons, increasing their diffuse scattering and consequently also the electrical

Table 1. Variation in electrical resistance (ΔR/R) of Au NW devices measured in air after exposure to alkanethiol solutions with different concentrations. The values of ΔR were calculated from the expression $\Delta R/R = (R_{mea}-R_{bi}/R_{bi}) \times 100$, where R_{bi} and R_{mea} are the resistance of NWs before and after immobilization of alkanethiol molecules, respectively. The variations in the values of ΔR/R correspond to the standard deviation of the mean with n=3 measurements from different devices.

ΔR / R (%)						
Organothiol	Thiolpropane		Mercapto-propionic acid		Cysteamine	
concentration / mmol L^{-1}	Air	Water	Air	Water	Air	Water
0.01	37.5 ± 6	21.6 ±8	37.5 ±5	31.4 ±7	30.1 ±7	54.5 ±7
0.1	44.4± 8	115.3±9	42 ±12	22.9 ±6	22.4 ±5	68.2 ±10
0.5	52.2±12	60.6±7	55.7±7	228.6±12	94.7 ±9	54.5 ±9
1	62.5±11	137.3±10	99.2 ±10	257.1 ±10	126 ±10	181.8 ±9
10	209.7±10	277.7±10	163 ±13	327.1 ±11	177.5 ±11	315.9 ±8

resistance of the wires, as was observed in Figure 5A-F. The covalent binding and/or the physical adsorption of chemical species on the surface of the NWs is also considered to be the main cause of the transition of the I – V curves of the devices from linear to quasi-linear. This effect was observed in the measured curves irrespective of the alkanethiol molecule employed and it was also seen during measurements with solutions of NaCl in the absence of organothiols adsorbed on the NWs (Figure S2, supporting information). This indicates that the phenomenon is a general aspect for adsorbates that strongly interact on Au surfaces (Cl^- ions in the case of NaCl and S-moiety in the case of alkanethiols). Previous experimental and theoretical research indicated that the adsorption and diffusion of impurities from the air into the subsurfaces of polycrystalline Au NWs can strongly affect the linear electrical behavior of NWs.[37,38] Since NWs with diameters of 2 nm have an extremely large surface area to volume ratio and the thiol moieties of the organothiols can interact strongly with Au NW surfaces, it is believed that the interaction and diffusion of these thiol moieties into subsurfaces of NWs can drastically increase electron scattering at the surface and thus cause the quasi-linear behavior observed in the I – V curves.

These effects were first described more than 50 years ago by Fuchs and Sondheimer for thin metal films and a more complete model was developed in the nineties by Persson.[33,39,40] Persson's model indicates that the diffuse scattering of carriers on surfaces is strongly related to the adsorbate-metal electronic interaction. That is to say, the increase in the adsorbate density of states at the Fermi energy level of Au leads to an increase in the resistance of the metal surface. This is an important feature when considering the electronic interactions between adsorbates and metals, since it implies that the driving force changing the resistance of the metal is mainly dominated by the HOMO-LUMO interaction resulting from the metal-adsorbate binding moiety.[40,41] Hence, Persson's model predicts that for sensors based on metal NWs, the resistance change is independent of the chain length or functional groups of the adsorbate that do not interact directly with the orbitals near the HOMO-LUMO gap. This effect was identified in X-ray photoelectron spectroscopy experiments, showing that the

energy binding of the thiol moiety from different thiolate molecules on Au surface was the same.[42] Additionally, Bohn's group demonstrated through a series of experiments employing alkanethiols with different lengths that the change in resistivity due to adsorption of molecules on ultrathin films of Au was independent of the length of the molecules.[43,44]

These observations help to explain the increase in the resistance of the NWs when the thiols bind on their surface, but it is clear that the environment in which the measurements are carried out also plays an important role as an additional source of electron scattering on the NW surface. Therefore, in the following we consider the resistance changes of the nanowires in solutions. The I–V characteristics of chemically modified NWs are very different in water-based measurements in comparison with air measurements and this must be influenced by the acid-base properties of the functional groups of the molecules immobilized on Au NWs. This observation is supported by the fact that all the measurements in water were performed in the absence of electrolytes, thus minimizing the contribution of electron transfer processes or dipole interactions from the adsorption of ions such as Na^+, K^+ or Cl^- on the NW surface. Control experiments in water show that the resistance of unmodified NWs is increased by about 5% in comparison to the resistance of the wires in air. In addition, no hysteresis effect was observed in the I–V curves of the NWs before their chemical modification. On the other hand, as already pointed out, the measured I–V curves of chemically modified NWs exhibited an interactive effect of surface chemistry and hysteresis. The top left inserts in Figures 5D-F show the zoomed I – V curves near 0 V of the Au NW devices modified with 10 µmol L^{-1} of TP, CA and MPA in comparison with their non-modified surface. Clearly, the hysteresis effect on the voltage scale is more pronounced on NW surfaces modified with MPA, which exhibited a voltage hysteresis width in the voltage range between forward and backward sweeps when the current was 0 A, of 75 mV in comparison to 20.1 mV and 15.7 mV presented by TP and CA, respectively. In addition, in all the three cases the I–V curves showed reproducible hysteresis at both positive and negative bias. A significant dependence of this hysteretic behaviour on the MPA concentration employed was also observed, with higher concentrations of MPA such as 10 mM L^{-1} producing hysteresis width near 0 V as large as 281 mV. On the other hand, the magnitude of the hysteresis of the devices functionalized with TP and CA showed a less pronounced concentration-dependence increase, with a maximum hysteresis width near 0 V of 47 mV and 42 mV when the devices were functionalized with 10 mM L^{-1} of TP and CA, respectively.

The observed hysteresis is associated with the charge in the functional groups of immobilized molecules and the existence of an environment reorganization process coupled to charge transport due to the electric-field-induced migration of mobile ions.

Indeed, besides the charges of the amine and carboxyl groups, the hydration of the substrate (SiO_2) and the NWs leads to the adsorption of surface charge traps around the NW surface. In fact, hysteresis due to charge trapping by water molecules in the electrical characteristics of other unidimensional nanomaterials such as carbon nanotubes, silicon and germanium nanowires has been previously reported.[45-47] In our case, a possible mechanism relies in the fact that before biasing the NW devices, the water molecules close to the self-assembled monolayers form an oriented dipole layer, in which their orientation and alignment is dependent on the surface chemistry/thiol functional group (Figure 6).[48,49] In the case of MPA and CA, the water molecules (including water charge traps) can interact and align themselves through dipole-dipole interactions with the carboxyl (Figure 6A) and the amine (Figure 6B) functional groups, respectively. In the absence of an externally applied electric field, these surface-orientated water molecules help to counter balance the charge of the fraction of carboxyl and amine groups that are ionized.

Meanwhile, in the case of TP, which does not have a polar functional group exposed to the surface, the water molecules close to the self-assembled monolayer may adopt a randomly orientated structure.

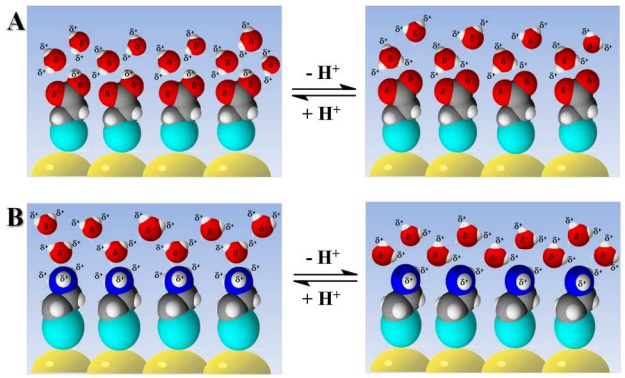

Fig. 6 Schematic illustration of the dependence of the orientation and alignment (based on dipole moment) of water molecules close to the self-assembled monolayers of A) MPA and B) CA as a function of their surface chemistry. The hydrogen atoms are represented by the white balls, while oxygen and nitrogen atoms are the red and blue balls, respectively. The cyan balls represent the sulfur moiety of the molecules binding to Au (yellow hemispheres).

With the application of a bias voltage sweep (V: $-V_{max} \rightarrow +V_{max} \rightarrow -V_{max}$), the resulting interfacial applied electric field influences the protonation/deprotonation of the functional groups of the immobilized alkanethiols and also the arrangement of the water molecules and trap states close to the surface.[49] For MPA, when the applied potential is negative, the deprotonated ($-COO^-$) fraction of the carboxyl groups decreases because the local activity of protons increases at the interface, as described by the Poisson-Boltzmann equation for the activity of ions at a charged interface[50]

$$a_{interface} = a_{bulk} \exp(-zF\Psi_s/RT) \qquad \text{(Eq. 1)}$$

where z is the charge of the ion and Ψ_s is the surface potential. In the case of protons, this relation predicts a change in the interfacial pH, where at more negative potentials the interfacial pH is lowered and the fraction of carboxylate anions decreases because of increased protonation. For CA, the more negative applied potentials can increase the rate of protonated primary amine groups. The sweeping to positive bias polarization causes the dynamic process of proton exchange between the functional

groups of MPA/CA and the water molecules immediately adjacent to the monolayers to continue. Therefore, at positive applied potentials the fraction of carboxylate anions and unprotonated primary amine groups from MPA and CA, respectively, should increase because the local activity of protons decreases at the interface. This influence of the acid-base chemistry of the functional groups of self-assembled monolayers on the interfacial electric characteristics of metal electrodes has already been observed.[51-54] However, to the best of our knowledge this is the first demonstration of the dependence of the electrical characteristics of metal NWs sensors as a result of the dipole of the functional groups of adsorbates. Such findings offer unique opportunities for nanoscale sensors based on ultrathin NWs because of their large surface area and interfacial engineering.

The fact that the largest hysteresis on the voltage scale was observed for surfaces modified with MPA, but not with those modified with CA, can be related to the fraction of ionized functional groups. The pK_a values for the carboxyl groups from MPA and primary amine groups from CA are 4.8 and 8.35, respectively.[55,56] This means, as expected, that in the pH range in which the experiments were carried out both functional groups of the molecules should be ionized. It is well known that in solutions the primary amine group of cysteamine is completely protonated when pH < 8.35. However, this situation can be totally different when these molecules are immobilized on surfaces due to their relatively dense packing arrangement. In this case, once a surface amine group is protonated, its positive charge can suppress the protonation of neighboring groups. The poor solvation and bridging between neighboring charged groups would also suppress further protonation. In the case of MPA, the carboxyl groups have a higher volume and their negative charge in pH > 4.8 can be stabilized by the formation of dimers on the surface. Indeed, this is consistent with other reports showing that the fraction of protonated amine groups of molecules immobilized on different surfaces in pH ≈ 7 was very low, and could be increased by at least 50 % in pH ≈ 1.[57-59] On the other hand, immobilized carboxylated molecules could represent a relatively higher fraction of ionization. The presence of these charges due to the protonation/deprotonation of the functional groups on the surface is directly related to the interfacial potential at the plane of the functional groups and can be probed by zeta potential (ζ-potential) measurements. Nevertheless, since it would be difficult to measure the ζ-potential on the surface of NW devices, we attempted to measure it by immobilizing 10 mmol L^{-1} of MPA, CA and TP on ultrathin Au NWs dispersed in solution (see Experimental). The results of these analyses demonstrated that in pH 6.7 the ζ-potential of carboxylated NWs was -40 ± 8.9 mV (negative due to the deprotonation), whereas those modified with cysteamine was only + 6 ± 6.5 mV (positive due to the protonation). In the case of the immobilization of TP molecules, which form a hydrophobic surface without ionizable groups, it was observed that as expected the ζ-potential exhibited a low magnitude (-5 ± 6.9 mV) in the range of negative potential. As the measurements were only performed in deionized water, this negative value for the zeta potential of TP is attributed to the adsorption of hydroxide ions generated from the self-ionization of water. These results clearly corroborate our previous observation about the protonation/deprotonation of the functional groups of the molecules analyzed, where it can be seen that for NWs modified with MPA the ζ-potential measured was about sixfold larger than for NWs modified with CA.

The surface charge density (σ) associated with the acid/base reaction was obtained by employing the Grahame equation (Eq. 3) [50]

$$\sigma = \sqrt{8\varepsilon\varepsilon_0 kTn_0}\,\sinh\left(\frac{\Phi_s}{2V_{th}}\right) \qquad \text{(Eq. 2)}$$

where ε is the dielectric constant of the medium, ε_0 is the dielectric permittivity of vacuum, k is the Boltzmann constant, T is the temperature, n_0 corresponds to the bulk ion concentration (in this case 0.2 μmol L^{-1}), V_{th} is the thermal voltage and Φ_s is the surface potential at the plane of the functional groups. The surface charge density value found for CA was 0.6 nC cm^{-2}, which was consistent with the notion that the fraction of ionized amine groups was low. On the other hand, for MPA a value of 4.2 nC cm^{-2} was determined for surface charge density.

To estimate the surface coverage and correlate it with the fraction of ionized functional groups, we applied Persson's model, which states that the resistance increase is linearly proportional to the coverage density. Thus, by taking into account the kinetic model described by Jung *et al.* for adsorption of alkanethiols on Au[60]

$$\theta_S = \theta_{S_{max}}\left[1 - \exp\left(-\frac{S_o C v t}{\theta_{S_{max}}}\right)\right] \qquad \text{(Eq. 3)}$$

where θ_S is the coverage density, t is the time, S_o is the probability that a molecule will be adsorbed upon its collision with the surface of the metal, θ_{Smax} is the full surface coverage per unit area, C is the concentration and v is molecular velocity. The following relation with Persson's model was established on the basis of the change in electrical resistance (ΔR)[19]

$$\frac{\Delta R}{R} = \left(\frac{\Delta R}{R}\right)_{max}\left[1 - \exp\left(-\frac{S_o C v t}{\theta_{S_{max}}}\right)\right] \qquad \text{(Eq. 4)}$$

Plots of ΔR/R measured in air to avoid contributions from water adsorbates versus C (Figure 7) for all three molecules showed an increase in the resistance of the NWs while increasing the density of adsorbates on their surfaces, as predicted by Persson's model.[40] These results show a linear increase in the electrical resistance of the NWs upon absorption from solutions up to 1 mmol L^{-1}, followed by saturation at higher value. We note that for absorption from solutions with relatively low concentrations (10 and 100 μmol L^{-1}) of alkanethiols, the electrical response of the devices is statistically similar. When the concentration was increased, differences in the electrical response of the devices were observed for the three alkanethiols, even when adsorbed from solutions having the same concentration. Variations on the surface coverage resulting from the packing density of the molecules due to lateral and vertical chemical interactions are well-known in bulk metal surfaces and are also a general feature of nanodevices. Similar observations have been made in carbon nanotubes, silicon and gold/copper surfaces.[61-63] In the linear range, a higher increase in electrical variation and thus a higher

sensitivity was observed for those NW devices covered by MPA, followed by CA and TP, respectively. When 10 mmol L^{-1} solutions were employed, the electrical response of the Au NW devices only showed a slight increase upon adsorption of the molecules. Applying the least squares method, these measured data were fitted with Eq. 4 adjusting t = 600 s (time that the NW devices were submerged in the alkanethiol solutions), S_o around 2 x 10^{-8} and v around 0.03 cm s^{-1}.[52] It was then possible to determine the total surface coverage per unit area for each surface as shown in Table 2. These data demonstrate that the maximum coverage density presents a small difference for all three molecules employed for immobilization onto NWs and are in agreement with other experimental studies for coverage of Au surfaces by alkanethiols with similar chain length.[60,64] The highest degree of coverage was obtained with TP, followed by CA and MPA, respectively. This tendency agrees well with previous surface plasmon resonance results, which demonstrates that organothiols with bulkier functional groups such as –COOH adsorbes more slowly on Au surface than their corresponding alkanethiol with $–CH_3$ group.[60] These results further indicate that TP and CA form layers with higher densities of molecules and better insulating properties with lower capacitance than MPA.

Based on the results of surface charge density calculated previously and the total surface coverage found from the fitted data, the fraction of ionized molecules was roughly estimated as 0.015% and 0.002%, for MPA and CA, respectively. These results are comparable to reported studies, which show that less than 1% of the carboxylic groups in self-assembled monolayers of 11-mercaptoundecanoic acid immobilized on Au (111) participate in the potential induced protonation/deprotonation process on the electrode surface. [53] These values demonstrate that even a relative small fraction of ionized species on the surface of NWs is able to cause a surface charging that can influence the electron transport of Au NWs in solution.

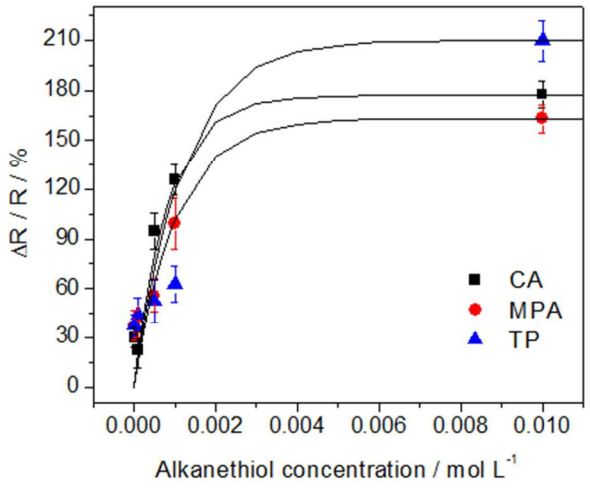

Fig. 7 Plots of ΔR/R as a function of alkanethiol concentration employed for immobilizing on Au NW devices. The dots correspond to the experimental data, whereas the solid lines are the fits of Eq. 4 for the adsorption of thiolpropane, mercapto-propionic acid and cysteamine. The data correspond to the measurements in air to avoid contributing to the resistance variation due to water adsorbates. The error bars correspond to the standard deviation in the values of ΔR for the mean with n=3 measurements.

Presumably, the ionization of the functional groups of assembled alkanethiols and the adsorption and ionic rearrangements induced by electric potentials through water molecules are mainly responsible for the drastic increase in the resistance of the nanowires when the measurements were carried out in solution.

Although Persson's model does not explain how this combined effect of thiol binding and surface charge of functional groups of immobilized molecules can influence the electron transport on metal surfaces in solution, these results clearly show that the electrical resistance of ultrathin Au NWs is extremely sensitive to the effects of molecular adsorption and the interfacial charge of the adsorbates. Although it should not be expected that the surface charge of adsorbates could influence the electrical properties of metal nanowires as they do in semiconductor materials, the small lateral size and the relatively long length of the ultrathin Au NWs make the pathway of their conducting electrons become more sensitive to the chemical influences of the environment. Thus, as the alkanethiol molecules have a short length, the surface charge imposed by their acid-base properties associated with the adsorption of water molecules through different dipole interactions could directly affect the electron scattering on the surface of nanowires during electrical measurements.

Table 2. Total surface coverage of Au NW devices modified with different alkanethiol molecules.

Molecule	Total Surface Coverage / molecules cm^{-2}
thiolpropane	2.16 x 10^{14}
mercapto-propionic acid	1.80 x 10^{14}
cysteamine	1.94 x 10^{14}

This study demonstrates the influence and the critical dependence of different chemical functionalizations in the electrical response of ultrathin metal NWs and can help to extend our understanding of their surface-sensitive resistivity change to develop a new concept of sensors based on ultrathin NW devices.

4 Conclusions

In summary, we demonstrate the synthesis and assembly of ultrathin single-crystalline Au NWs into functional nanodevices, i.e. chemiresistors, in which the electrical response to the adsorption of small alkanethiol molecules with different functional groups was investigated. Specifically, we show that the binding of organothiols on ultrathin Au NWs resulted in a concentration-dependent resistance increase in the devices, with a remarkable change in resistance of over 100% when the NWs were exposed to a few millimoles of the respective molecules. The measurements in solution are of particular interest, where the acid-base properties of the immobilized molecules have a significant impact on the electrical transport through ultrathin

NWs. These results demonstrate the critical dependence of sensitivity on the head group of the adsorbed molecules and thus provide fundamental insights into the electrical response of ultrathin metal NWs in solution. Moreover, our data suggest the applicability of this experimental design for characterizing the interfacial properties on the surface of nanoelectrodes of comparable size to the electrochemical double layer. These findings open up new opportunities for metal NW-based chemiresistors and can help to develop highly sensitive sensors to readily probe low concentrations of specific analytes that are able to interact with the dipoles of the functional groups of immobilized molecules.

Acknowledgements

This work was supported by a research grant provided by the DFG research training group "Biointerface" at RWTH Aachen University.

Notes and references

[a] *Peter Grünberg Institut-8, 2Peter Grünberg Institut-5, Forschungszentrum Jülich GmbH, 52425 Jülich, Germany. Fax: +49 2461 61-8733; Tel: +49 2461 61-2364; E-mail: kisner.alexandre169@gmail.com, y.mourzina@fz-juelich.de*
[b] *Jülich Aachen Research Alliance (JARA)-Fundamentals of Future Information Technology, 52425 Jülich, Germany.*
[c] *Peter Grünberg Institut-5, Forschungszentrum Jülich GmbH, 52425 Jülich, Germany.*
[d] *Institute of Inorganic Chemistry, RWTH Aachen University, Landoltweg 1, 52074 Aachen, Germany.*

† Electronic Supplementary Information (ESI) available: [current-voltage characteristics of Au NW devices modified with organothiols and measurements in salted solutions]. See DOI: 10.1039/b000000x/

‡ Current address: Department of Cell Biology and Neuroscience, Rutgers University, 604 Allison Road, Piscataway, NJ 08854-8082.

1 J. Kong, N. Franklin, C. Zhou, S. Peng, J. J. Cho and H. Dai, *Science*, 2000, **287**, 622.
2 R. Yu, C. Pan and Z. Lin Wang, *Energy Environ. Sci*., 2013, **6**, 494.
3 B. Wang, L. F. Zhu, Y. H. Yang, N. S. Xu and G. W. Yang, *J. Phys. Chem. C*, 2008, **112**, 6643.
4 E. Stern, J. F. Klemic, D. A. Routenberg, P. N. Wyrembak, D. B. Turner-Evans, A. D. Hamilton, D. A. LaVan, T. M. Fahmy and M. A. Reed, *Nature*, 2006, **445**, 519.
5 Y. Engel, R. Elnathan , A. Pevzner , G. Davidi , E. Flexer and F. Patolsky, *Angew. Chem. Int. Ed.*, 2010, **49**, 6830.
6 F. Patolsky, G. Zheng and C. M. Lieber, *Anal. Chem*., 2006, **78**, 4260.
7 I. M. Feigel, H. Vedala and A. Star, *J. Mater. Chem*., 2011, **21**, 8940.
8 R. M. Penner, *Annu. Rev. Anal. Chem*., 2012, **5**, 461.
9 H. He and N. J. Tao, *Adv. Mater*., 2002, **14**, 161.
10 Z. Liu and P. C. Searson, *J. Phys. Chem. B*, 2006, **110**, 4318.
11 C. Z. Li and N. J. Tao, *Appl. Phys. Lett*., 1998, **72**, 894.
12 C. Z. Li, A. Bogozi, W. Huang and N. J. Tao, *Nanotechnology*, 1999, **10**, 221.
13 C. Z. Li, H. X. He, A. Bogozi, J. S. Bunch and N. J. Tao, *Appl. Phys. Lett*., 2000, **76**, 1333.
14 B. Xu, H. X. He and N. J. Tao, *J. Am. Chem. Soc*., 2002, **124**, 13568.
15 P. Shi, J. Y. Zhang, H. Y. Lin and P. W. Bohn, *Small*, 2010, **6**, 2598.
16 K. Dawson, J. Strutwolf, K. P. Rodgers, G. Herzog, D. W. M. Arrigan, A. J. Quinn and A. O'Riordan, *Anal. Chem*., 2011, **83**, 5535.
17 F. Favier, E. C. Walter, M. P. Zach, T. Benter and R. M. Penner, *Science*, 2001, **293**, 2227.
18 F. Yang, K. C. Donavan, S.-C. Kung and R. M. Penner, *Nano Lett*., 2012, **12**, 2924.
19 H.-Y. Lin, H.-A. Chen and H.-N. Lin, *Anal. Chem*., 2008, **80**, 1937.
20 A. Halder and N. Ravishankar, *Adv. Mater.*, 2007, **19**, 1854.
21 C. Wang, C. Hu, C. M. Lieber and S. Sun, *J. Am. Chem. Soc*., 2008, **130**, 8902.
22 X. Lu, M. S. Yavuz, H. Y. Tuan, B. A. Korgel and Y. Xia, *J. Am. Chem. Soc*., 2008, **130**, 8900.
23 N. Pazos-Prez, D. Baranov, S. Irsen, M. Hilgendorff, L. M. Liz-Marzán and M. Giersig, *Langmuir*, 2008, **24**, 9855.
24 Z. Huo, C. K. Tsung, W. Huang, X. Zhang and P. Yang, *Nano Lett.*, 2008, **8**, 2041.
25 A. Kisner, M. Heggen, E. Fernández, S. Lenk, D. Mayer, U. Simon, A. Offenhäusser and Y. Mourzina, *Chem. Eur. J*., 2011, **17**, 9503.
26 B. Wang, and H. Haick, *ACS Appl. Mater. Interf.*, 2013, **5**, 2289.
27 B. Wang, and H. Haick, *ACS Appl. Mater. Interf.*, 2013, **5**, 5748.
28 M. Y. Bashouti, R. T. Tung and H. Haick, *Small*, 2009, **5**, 2761.
29 R. Haight, L. Sekaric, A. Afzali and D. Newns, *Nano Lett.*, 2009, **9**, 3165.
30 M. Vosgueritchian, M. C. LeMieux, D. Dodge, and Z. Bao, *ACS Nano*, 2010, **4**, 6137.
31 U. Chandni, P. Kundu, A. K. Singh, N. Ravishankar and A. Ghosh, *ACS Nano*, 2011, **5**, 8398.
32 S. Pud, A. Kisner, M. Heggen, D. Belaineh, R. Temirov, U. Simon, A. Offenhäusser, Y. Mourzina and S. Vitusevich, *Small*, 2013, **9**, 846.
33 E. Sondheimer, *Adv. Phys.*, 1952, **1**, 1.
34 J. C. Love, L. A. Estroff, J. K. Kriebel, R. G. Nuzzo and G. M. Whitesides, *Chem. Rev.*, 2005, **105**, 1103.
35 C. D. Bain, E. B. Troughton, Y. T. Tao, J. Evall, G. M. Whitesides and R. G. Nuzzo, *J. Am. Chem. Soc*., 1989, **321**, 111.
36 W. Lee and M. Hara, H. Lee, *Mat. Sci. Eng. C*, 2004, **24**, 315.
37 C. M. Lilley and Q. Huang, *Appl. Phys. Lett*., 2006, **89**, 203114.
38 C. M. Lilley and R. Meyer, *Bull. Pol. Ac. Tech*., 2007, **55**, 187.
39 K. Fuchs, *Proc. Cambridge Philos. Soc*., 1938, **34**, 100.
40 B. N. J. Persson, *Phys. Rev. B*, 1991, **44**, 3277.
41 B. K. Duan, J. Zhang and P. W. Bohn, *Anal. Chem*., 2012, **84**, 2.
42 T. Ishida, N. Choi, W. Mizutani, H. Tokumoto, I. Kojima, H. Azehara, H. Hokari, U. Akiba and M. Fujihira, *Langmuir*, 1999, **15**, 6799.
43 Y. Zhang, R. H. Terrill and P. W. Bohn, *J. Am. Chem. Soc*., 1998, **120**, 9969.
44 Y. Zhang, R. H. Terrill and P. W. Bohn, *Anal. Chem*., 1999, **71**, 119.
45 W. Kim, A. Javey, O. Vermesh, Q. Wang, Y. Li and H. Dai, *Nano Lett.*, 2003, **3**, 193.
46 Y. Paska and H. Haick, *ACS Appl. Mater. Interf.*, 2012, **4**, 2604.
47 D. Wang, Y.-L. Chang, Q. Wang, J. Cao, D. B. Farmer, R. G. Gordon and H. Dai, *J. Am. Chem. Soc.*, 2004, **126**, 11602.
48 N. Goutev and M. Futamata, *Appl. Spectrosc*., 2003, **57**, 506.
49 Z. D. Schultz, S. K. Shaw and A. A. Gewirth, *J. Am. Chem. Soc*., 2005, **127**, 15916.
50 A. J. Bard and L. R. Faulkner, Electrochemical Methods: Fundamentals and Applications; John Wiley and Sons: New York, 2000.
51 C. P. Smith and H. S. White, *Langmuir*, 1993, **9**, 1.
52 I. Burgess, B. Seivewright and R. B. Lennox, *Langmuir*, 2006, **22**, 4420.
53 A. M. Luque, W. H. Mulder, J. J. Calvente, A. Cuesta and R. Andreu, *Anal. Chem.*, 2012, **84**, 5778.
54 C. Ma and J. M. Harris, *Langmuir*, 2011, **27**, 3527.
55 J. Zhao, L. Luo, X. Yang, E. Wang and S. Dong, *Electroanal.*, 1999, **11**, 1108.
56 C. E. Housecroft and A. G. Sharpe, Inorganic Chemistry (3rd ed.). Prentice Hall. Chapter 6: Acids, Bases and Ions in Aqueous Solution, 2008.
57 W. –C. Lin, S. –H. Lee, M. Karakachian, B. –Y. Yu, Y. –Y. Chen, Y.-C. Lin, C.-H. Kuo and J. –J. Shyue, *Phys. Chem. Chem. Phys*., 2009, **11**, 6199.
58 Y.-C. Lin, B. -Y. Yu, W.-C. Lin, S.-H. Lee, C.-H. Kuo and J. -J. Shyue, *J. Colloid Interface Sci*., 2009, **340**, 126.
59 J. -J. Shyue, M. R. De Guire, T. Nakanishi, Y. Masuda, K. Koumoto and C. N. Sukenik, *Langmuir*, 2004, **20**, 8693.
60 L. S. Jung and C. T. Campbell, *J. Phys. Chem. B*, 2000, **104**, 11168.

61 Y. Zilberman, U. Tisch, G. Shuster, W. Pisula, X. Feng, K. Mullen, and H. Haick, *Adv. Mater.* 2010, **22**, 4317.
62 N. Gozlan and H. Haick, *J. Phys. Chem. C*, 2008, **112**, 12599.
63 N. Gozlan, U. Tisch, H. Haick, *J. Phys. Chem. C*, 2008, **112**, 12988.
64 L. S. Jung and C. T. Campbell, *Phys. Rev. Lett.*, 2000, **84**, 5164.

